High-molecular-weight dissolved organic matter enhanced phosphorus availability in paddy soils: Evidence from field and microcosm experiments

Hai-Bo Wang , Xi-Peng Liu , Bing-Jie Jin , Yu-Chen Shu , Cheng-Liang Sun , Yong-Guan Zhu , Xian-Yong Lin *

Posted Date: 3 October 2023

doi: 10.20944/preprints202309.2078.v1

Keywords: Soil phosphorus availability; Dissolved organic matter; Organic fertilizer; Competitive adsorption; Molecular weight

Article

High-Molecular-Weight Dissolved Organic Matter Enhanced Phosphorus Availability in Paddy Soils: Evidence from Field and Microcosm Experiments

Hai-Bo Wang [1], Xi-Peng Liu [2], Bing-Jie Jin [3,4], Yu-Chen Shu [1], Cheng-Liang Sun [1], Yong-Guan Zhu [1,3] and Xian-Yong Lin [1,*]

[1] MOE Key Laboratory of Environment Remediation and Ecological Health, College of Environmental and Resource Sciences, Zhejiang University, Hangzhou 310058, PR China.
[2] Microbial Ecology cluster, Genomics Research in Ecology and Evolution in Nature (GREEN), Groningen Institute for Evolutionary Life Sciences (GELIFES), University of Groningen, 9747 AG Groningen, The Netherlands
[3] Key Lab of Urban Environment and Health, Institute of Urban Environment, Chinese Academy of Sciences, Xiamen 361021, PR China
[4] Yangtze Delta Region Healthy Agriculture Institute, Jiaxing 314500, PR China
* Correspondence: author: Xian-Yong Lin, College of Environmental and Resource Sciences, Zhejiang University, Hangzhou, 310058, China; E-mail: xylin@zju.edu.cn, Tel: +86-571-88982476, Fax: +86-571-86971395

Abstract: Dissolved organic matter (DOM) derived from organic fertilizers may increase soil phosphorus (P) availability. However, the frequently observed correlation between soil P availability and dissolved organic carbon (DOC) content has led to an excessive focus on DOC content at the expense of DOM properties. The present study investigated the influence of DOM characteristics on soil P availability by using a 6-year field experiment and microcosms of P sorption in paddy soil. Our results showed that partial replacement of chemical P fertilizer with manure or crop straw increased P fertilizer-use efficiency, even when decreasing chemical P input by 34 %, compared to normal chemical fertilization. The microcosm experiment demonstrated that DOM properties, rather than total DOC content, determine soil P sorption capacity, despite the significant correlation between DOC content and P availability observed in the field experiment. Manure-DOM exerted stronger inhibitory effects on P sorption than straw-DOM, and high molecular weight (HMW)-fractionated DOM exerted stronger inhibitory effects on P sorption than low-molecular-weight-fractionated DOM by 16-20%. The mechanism was rooted in the HMW DOM with unique characteristics (e.g., strong aromaticity, hydrophobicity, abundant humic-like components, carboxyl groups, and benzene ring structures) competing for soil P sorption sites (e.g., reduction in specific surface area and micropore volume), decreasing the soil surface charge (e.g., zeta potential), and thereby suppressing P sorption in paddy soil. Our study points out a promising avenue for regulating organic matter properties with organic fertilization to improve P use efficiency in agricultural soils.

Keywords: soil phosphorus availability; dissolved organic matter; organic fertilizer; competitive adsorption; molecular weight

1. Introduction

Phosphorus (P) is a critical nutrient that influences crop growth and yield. High P sorption and fixation in soil often leads to low P fertilizer-use efficiency (PUE), although large quantities of chemical P fertilizer have been applied to agricultural soils (Zhu et al., 2018; Zou et al., 2022). However, chemical P fertilizers derived from phosphate rocks are finite resources. It is projected that commercially exploitable phosphate rock will be exhausted within decades (Cordell et al., 2009; Van Vuuren et al., 2010), which could prevent farmers from achieving stable yields through the application of high amounts of chemical P fertilizers. Moreover, high P accumulation in the soil owing to low PUE may lead to water eutrophication (Cordell and White, 2014; Mekonnen and

 doi:10.20944/preprints202309.2078.v1

Hoekstra, 2018). Consequently, it is critical to formulate better management practices to improve P use efficiency in crops for sustainable agricultural management.

Enhancing P availability for plants can be achieved by regulating soil organic carbon (SOC), which represents a promising strategy without excessive chemical P inputs (Borges et al., 2019; Qaswar et al., 2020). This has been indicated by numerous field and greenhouse experiments where the organic–inorganic fertilizer application promoted P uptake by crops and increased crop yield (Du et al., 2020; Hawkins et al., 2022; Nobile et al., 2020; Romanyà et al., 2017; Takahashi and Katoh, 2022; Yan et al., 2013). The beneficial effect of organic fertilizer on P availability is mainly considered deriving from the organic matters introduced. On the one hand, organic matter may influence P fractions and mobilization in the soil by altering soil physicochemical properties or microbial activity, such as pH and phosphatase activity (Bi et al., 2020; Cong and Merckx, 2005; Nobile et al., 2020; Qaswar et al., 2020). On the other hand, organic matters are likely to compete with P for sorption sites on the surface of soil mineral particles, leading to higher P availability (Borges et al., 2019; Perassi and Borgnino, 2014; Ström et al., 2002). A recent study suggests that the accumulated P in the soil can be bioavailable to crops for several years to decades with the mobilization of soil organic matters (Hawkins et al., 2022). Therefore, these results support the utilization of organic fertilizers for improving P use efficiency and deliver a hypothesis that an equal or even better crop yield is highly possible after applying organic matters even when reducing chemical P inputs to a certain extent.

Dissolved organic matter (DOM) followed by organic amendments in soil could be a key factor influencing P sorption and availability (Hunt et al., 2007; Li et al., 2022a; Mastný et al., 2018; Weyers et al., 2017). Many field studies found that organic fertilizer application increased both DOM content and P absorption by plants by attributing the key reason affecting P sorption capacity and availability to the elevated soil DOC content (Giesler et al., 2005; Liu et al., 2019b; Moorberg et al., 2017; Nobile et al., 2020; Yan et al., 2013). Indeed, some microcosm experiments have also shown that increasing the content of organic acids or organic fertilizer leachates leads to more P resolution from soil or minerals, indicating the direct effect of DOM content/concentration on P availability (Hou et al., 2018; Weyers et al., 2017; Zhu et al., 2021). However, recent studies have explored the inhibitory effects of various DOMs on the mineral-water interface interactions and suggested that DOM characteristics, such as molecular weights (MW) and humification degree, largely influence P sorption capacity of iron minerals (Chasse and Ohno, 2016; Deng et al., 2019; Li et al., 2022a; Lin et al., 2017; Takahashi and Katoh, 2022). Overall, these studies suggested two potential strategies of regulating soil P availability by using organic fertilizers and thereby contributing sustainable P management in soil. Despite this, a comprehensive understanding of how DOM contents and characteristics influence P immobilization in manured soil is still lacking, which may weaken the application efficacy of organic fertilizers in the field, leading to the waste of organic resources or unanticipated pollution.

DOM is characterized by a wide range of molecular weights, comprising low-MW (LMW) components (e.g., carbohydrates, sugars, and amino acids) and high-MW (HMW) substances (e.g., polyphenols, polycyclic aromatics, and humic substance) (Wu et al., 2020; Wu et al., 2021b). Both LMW and HMW components may influence adsorption properties of minerals owing to similar mechanisms such as altering pH, inhibiting hydroxyapatite precipitation, forming organic ligands, and competing for sorption sites (Ge et al., 2020; Hiemstra et al., 2013; Jalali and Jalali, 2022; Teng et al., 2020; Yuan et al., 2022; Zhu et al., 2021). Recent explorations on paddy and calcareous soils showed that the maximum P adsorption capacity of soil was significantly negatively correlated with DOM humification degree (Li et al., 2022a; Zhang et al., 2022). The highly humified DOM tends to be composed of HMW substances (Bolan et al., 2011; Nebbioso and Piccolo, 2013), implying the potential of HMW DOM on P sorption competition. However, the direct evidence linking the MW of DOM and soil P availability and immobilization following organic fertilizer application is still lacking.

Herein, we investigated (i) the effect of DOM content and properties on soil P availability based on a 6-year field experiment in paddy soil, and (ii) the mechanism by which exotic MW-fractionated DOM influences soil P availability using a soil microcosm experiment. We hypothesized that DOM properties influence soil P sorption capacity and that HMW DOM has better P improvement potential than LMW DOM in paddy soils after organic fertilizer applications.

 doi:10.20944/preprints202309.2078.v1

2. Materials and methods

2.1. Field experiment

To demonstrate that whether partial substitution of chemical P fertilizer with manure or crop straw could maintain high soil P availability despite a decrease in total P input, a 6-year field experiment was conducted under a rice–wheat rotation system with different fertilization regimes in 2016. The study site was located in the town of Si' an, Changxing County, Zhejiang Province, China (30°54′11″N, 119°37′26″E). The area has a subtropical humid monsoon climate with an annual temperature of 15.6 °C and 1309 mm of precipitation. The physicochemical properties of soil were provided in Supplementary Materials Text S1. Four fertilization regimes were included: (1) CK, control without fertilizer; (2) NPK, chemical fertilizers input with normal NPK doses; (3) OM, reducing chemical fertilizers P by 34% compared to NPK treatment and replacing 22% of the chemical P with organic manure P made the final total P dose 88% of that of the NPK treatment with the same total NK doses as the NPK treatment; (4) CS, reducing chemical fertilizers P by 34% compared to NPK treatment and applying 1500 kg / hm^2 of straw organic carbon, with the same amount of N, P, and K dose as the OM treatment (see Supplementary Table S1 for total nutrient input of each treatment). The experiment was conducted based on a completely randomized block design, with three replicates, and each block measuring 42 m^2.

Chemical fertilizers for N, P, and K were urea, calcium-magnesium phosphate, and potassium chloride, respectively. The organic fertilizers tested were commercial organic manure and crop straw (rice straw and wheat straw). For the CS treatment, wheat straw was applied during rice planting and rice straw was applied during wheat planting. The straw was returned to the field after shredding (approximately 10 cm in length), which is consistent with the actual straw return during production.

Soil samples were obtained by mixing five separate soil cores (0–20 cm) from each plot after crop harvest in November 2021. Air-dried soil was ground to pass through a 2-mm sieve before analysis.

The air-dried and sieved soil of every plot was used to evaluate P sorption isotherms. Briefly, soil (2 g) was shaken in 20 mL KCl solution (0.01 mol·L^{-1}) with final P concentrations of 0, 5, 10, 20, 40, 60, 80, 120, and 160 mg·L^{-1} for 24 h at 25°C. Three drops of chloroform were added to each tube to suppress microbial activity. The suspensions were centrifuged (3000 x g for 10 min) and filtered using a 0.45-μm membrane filter. The P concentrations were measured using the molybdate blue method, and the amount of P adsorbed to the soil was calculated based on the difference between initial P concentrations and equilibrated P concentrations. The maximum P sorption capacity (Q_m) and P bonding energy constant (k) represent P sorption capacity and P bonding energy at the sorption sites, respectively, calculated based on the Langmuir model (Supplementary Materials Text S2).

2.2. Soil microcosm experiment applied with MW-fractionated DOMs

To evaluate the effect of different MW-fractionated DOMs on soil P sorption capacity, batch sorption experiments were conducted to measure the P sorption capacity of soil with the addition of exogenous DOM solutions. DOMs derived from organic manure and crop straw are referred to as M-DOM and S-DOM, respectively. The MW-fractionated DOM samples were prepared using ultrafiltration cup technology instrument equipped with a 1 kDa membrane, as described by (Xu and Guo, 2017). The permeate solutions represented the LMW-fractionated DOM (<1 kDa), whereas the retentates were diluted to the initial volume and considered the HMW-fractionated DOM (1 kDa–0.45 μm). The LMW and HMW fractions of DOMs derived from organic manure and crop straw were named M-LMW, M-HMW, S-LMW, and S-HMW, respectively. This experiment collected soil from the field under the CK treatment. 2 grams of soil were added with 20 ml MW-fractionated DOM solutions where the concentration of different DOMs was adjusted to 60 mg C L^{-1}. The P isothermal sorption of DOM-treated soils was studied with final P concentrations of 0, 5, 10, 20, 40, 60, 80, 120, 160, and 200 mg L^{-1}. The adsorption isotherm experiments were conducted as described above with modifications: The final P concentrations of phosphate solution were calculated based on the P_i concentrations in the DOM solutions (P_o hydrolysis was minor and negligible). The pH of the mixture

was adjusted to 7.0 using 1 mol L^{-1} HCl and 1 mol L^{-1} NaOH, and the mixture was shaken at 4°C for 24h, instead of dropping chloroform, to inhibit microbial activity.

2.3. Physicochemical analyses of soil samples

Soil pH was measured in a 1:5 (w/v) mixture using a glass electrode. SOC concentration was determined by dichromate oxidation (Nelson and Sommers, 1996). Ammonium oxalate extractable Fe (Fe_{ox}), ammonium oxalate extractable aluminum (Al_{ox}), and ammonium oxalate extractable P (P_{ox}) were extracted using the method described in (Yan et al., 2013) and measured by inductively coupled plasma-optical emission spectroscopy (ICP-OES, Optima 8300, PerkinElmer, USA).

Soil Olsen-P was determined using the Olsen method (Olsen, 1954). Soil total P (TP) was extracted using the H_2SO_4–$HClO_4$ digestion method and determined using the molybdenum blue method. To eliminate the effect of the P application rate, used the Olsen-P to TP ratio (defined as the P activation coefficient, PAC) to better understand the difficulty of transformations between available P and total P after different fertilization regimes (Wu et al., 2017). A higher PAC indicates that more P is available to promote plant growth (Yang et al., 2019). The degree of P saturation (DPS) was calculated as the ratio of P_{ox} to the sum of Fe_{ox} and Al_{ox}, indicating the leaching potential of soil P (Hawkins et al., 2022). Soil P pools were sequentially fractionated using a modified Hedley method (Hedley et al., 1982; Tiessen and Moir, 1993) to obtain the H_2O-P, $NaHCO_3$-P, NaOH-P, and HCl-P pools in both the P_i (inorganic P) and P_o (organic P) fractions. The remaining soil residue was digested with perchloric acid to determine residual P. Specifically, H_2O-P, $NaHCO_3$-P_i, and $NaHCO_3$-P_o are soil labile P pools, whereas $NaHCO_3$-P_o and NaOH-P_o represent organic P pools. NaOH-P_i and HCl-P are Fe/Al hydroxide-associated P and calcium (Ca)-bound P, respectively. Residual P represents occluded P, which has the lowest plant availability.

2.4. Plant yield and P uptake

Rice grains were collected from each plot after threshing and air-dried to determine grain yield in November 2021. Seedling P uptake and P fertilizer use efficiency (PUE, the ratio of productive P output to P input) are described in our previous study (Li et al., 2022a). Briefly, 10 mature rice plants were harvested from each plot, manually divided into straw and grain after drying for 72 h at 65°C, and used to calculate ratio between straw and grain. The P concentrations in the straw and grain samples were measured and used to assess P absorbed by the plants.

2.5. DOM extraction and characterization

Dissolved organic matter derived from soil samples, organic manure, and crop straw were prepared as described in Li et al. (2022a). DOM concentration was expressed as DOC and determined using a Total Organic carbon analyzer (TOC-L, Shimadzu, Japan).

Ultraviolet (UV)-visible spectroscopy (UV-vis) and excitation-emission matrix (EEM) fluorescence spectroscopy were used to characterize the properties and compositions of the DOM samples. Fourier-transform infrared (FTIR) spectra of freeze-dried DOM solid samples were examined in the 400–4000 cm^{-1} range using FTIR spectroscopy (FT-IR iN10, Thermo Scientific Nicolet, USA). The UV absorbance at 254 nm ($SUVA_{254}$) and 260 nm ($SUVA_{260}$) were calculated as 100 times the ratio of UV-vis absorbance to the concentration of DOC at each wavelength, as indicators of aromaticity and hydrophobicity, respectively. The ratio of the slope (S_R; 275–295 nm slope: 350–400 nm slope) has previously been found to be negatively correlated with DOM molecular weight (Helms et al., 2008). The humification index (HIX) was used to reflect the humification degree of DOM (Zsolnay et al., 1999). Fluorescence index (FIX) has long been considered an index for differentiating between terrestrial and microbial DOM (McKnight et al., 2001). The methods for calculating the indicators are presented in Supplementary Materials Text S3. EEM coupled with parallel factor analysis (EEM-PARAFAC) modeling was performed using the OMFluor toolbox in MATLAB 2017a (MathWorks, Natick, MA, USA) to group and identify fluorescent components (Stedmon and Bro, 2008). More details about DOM characterization are presented in Supplementary Materials Text S4.

The EEM fluorescence spectroscopy combined with the PARAFAC model identified three fluorescence components (C1, C2, and C3) of paddy soil DOM under the different fertilization regimes (Fig. S1a, b). C1 (Ex/Em = 270/485 nm) has been reported to be a terrestrial humic compound consisting of highly aromatic organic compounds, is classified as a humic-like peak C. (Amaral et al., 2016; Lapierre and del Giorgio, 2014; McKnight et al., 2001). C2, with the most intense peak A (Ex/Em = 230/430), has been defined as "terrestrial humic-like" material (Panettieri et al., 2020; Romero et al., 2017; Ryan et al., 2022), and is enriched with fulvic acids (Yamashita et al., 2010). C3 (Ex/Em = 200(270)/295 nm) is an analogue of a tyrosine-like substance (Liu et al., 2018; Romero et al., 2017). In the MW-fractionated DOM, four components were successfully identified (Fig. S3a, b). The C1, C2, and C3 components were consistent with the DOM components in the field experiments. C4 (Ex/Em = 225(275)/340 nm) was assigned to the tryptophan-like peak T (Pitta and Zeri, 2021; Stedmon and Markager, 2005).

2.6. Microstructure analysis of soil coated with MW-fractionated DOM

The surface morphology of soil coated with MW-fractionated DOM was analyzed under Scanning Electron Microscopy (SEM) as described in Wu et al. (2021a). The specific surface area (SSA), total pore volume (V_{total}), micropore volume (V_{micro}), mesopore volume (V_{meso}), and average pore size (APS) were determined using the BET nitrogen sorption method using a Micrometrics ASAP 2020 surface area and porosity analyzer (Norcross, GA, USA). The zeta potential of soil before and after the addition of MW-fractionated DOM was measured at different pH values to investigate changes in the soil surface charge (Perassi and Borgnino, 2014).

2.7. Statistical analysis

One-way analysis of variance was performed using Tukey tests in IBM SPSS Statistics 20 (IBM Corp., Armonk, NY, USA) to identify significant differences between means at $P < 0.05$. The mean ± standard deviation of soil properties (pH, SOC, DOC, Fe_{ox}, Al_{ox}, P_{ox}, TP, and DPS), grain yield, seedling P uptake, and DOM spectral characteristics were determined. The relationships between the soil properties and DOM properties were evaluated using Pearson's correlation analysis. Redundancy analysis (RDA) was implemented using CANOCO v5.0 (http://www.canoco5.com/) to evaluate the effects of soil physicochemical properties and soil DOM properties on soil P sorption parameters. Partial least squares path modeling (PLS-PM) was conducted using the "plspm" R package to clarify the cascading pathways of DOM molecular weight on P availability. The validity of PLS-PM was evaluated by Goodness of fit and average variance extracted (AVE), both of which fitted the acceptable standards (Goodness of fit >0.7, AVE > 0.5). Other statistical analyses were performed in R v.4.0.4 (R Foundation for Statistical Computing, Vienna, Austria).

3. Results

3.1. Soil physicochemical properties, grain yield, and phosphorus availability in the field experiment

Different fertilization regimes influenced soil pH, SOC, DOC, P_{ox}, and TP concentrations considerably (Table 1). The soil pH in the NPK and OM treatments were significantly higher than that in the CK treatment ($P < 0.05$, Table 1). SOC and DOC concentrations in the OM and CS treatments were significantly higher than those in the CK and NPK treatments ($P < 0.05$, Table 1). In addition, TP concentrations (753.4 $mg \cdot kg^{-1}$) in the NPK treatment were significantly higher than those in the other treatments ($P < 0.05$, Table 1). DPS values of the fertilization treatments (NPK, OM, and CS) were significantly higher than those of the CK treatment ($P < 0.05$, Table 1). No significant differences in Fe_{ox} and Al_{ox} concentrations were observed among the treatments (Table 1).

Organic–inorganic fertilizations maintained high soil P availability for crops. Although the TP concentrations were lower than those in the NPK treatment, the organic–inorganic fertilization treatments (OM and CS) maintained high level of grain yield, seedling P uptake, and soil Olsen-P concentrations similar to the NPK treatment (Table 1, Fig. 1a). PAC values of soil amended with organic fertilizers were significantly larger than those of other soil samples, and were ranked as

Preprints (www.preprints.org) | NOT PEER-REVIEWED | Posted: 3 October 2023 doi:10.20944/preprints202309.2078.v1

follows: OM > CS > NPK > CK ($P < 0.05$, Fig. 1b). PUE values of the OM and CS treatments were 26.74% and 21.10% higher than those of the NPK treatment, respectively (Fig. 1c).

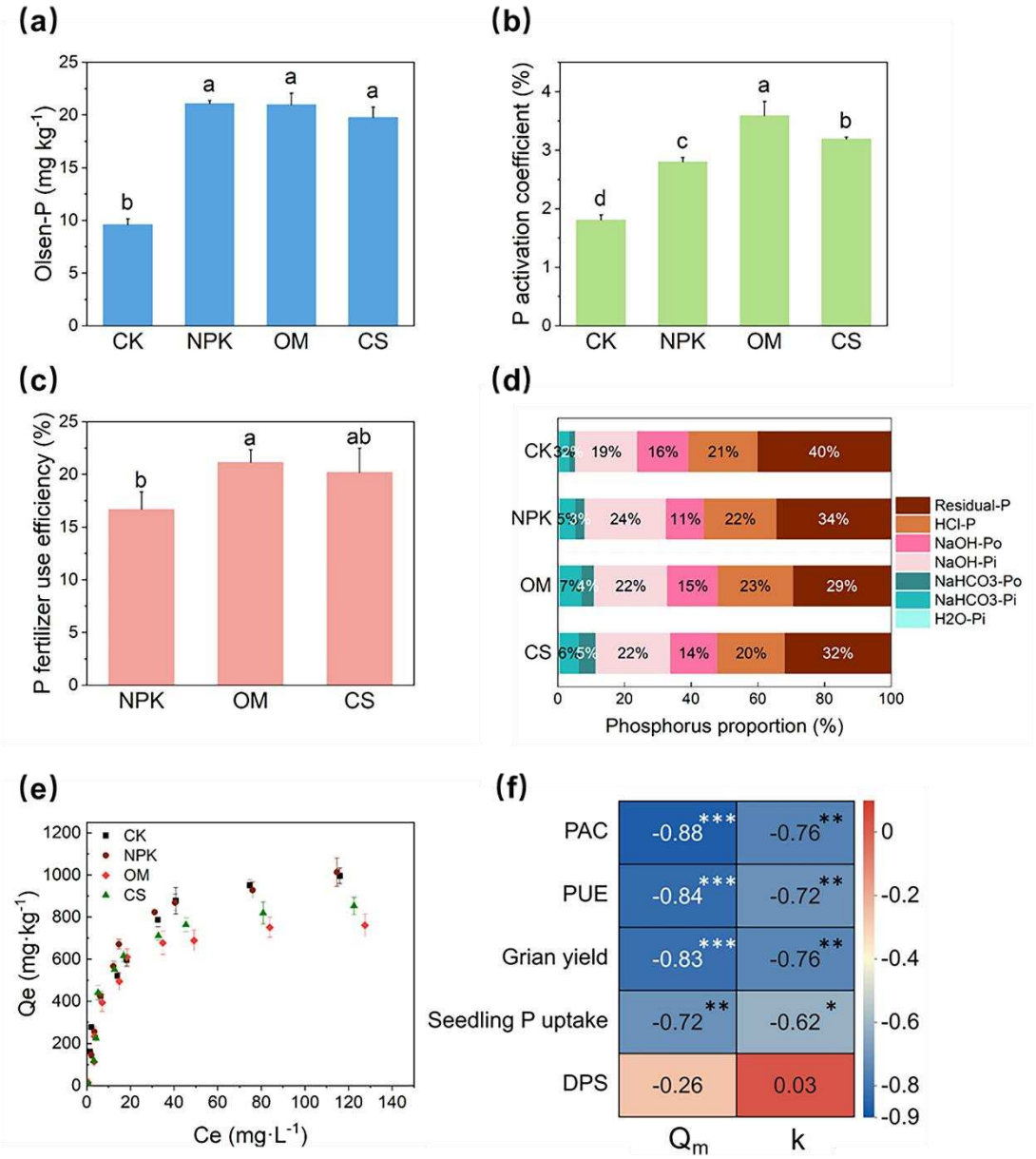

Figure 1. Phosphorous (P) fractions and availability in the paddy soil under different fertilization treatments. (a) Olsen-P, (b) P activation coefficient (PAC), (c) P fertilizer use efficiency (PUE), (d) proportions of each P fraction, and (e) P sorption isotherm of the paddy soils under different fertilization regimes. Different letters represent significant differences at $P < 0.05$ (Tukey's test). Error bars show standard deviations from triplicate measurements. (f) Correlation heatmap presenting the Spearman correlation coefficient (red represents positive correlation and blue represents negative correlation, $*$ $P < 0.05$, $**$ $P < 0.01$, and $***$ $P < 0.001$) of P activation coefficient, PUE, grain yield, seedling P uptake with Q_m and k.

Table 1. Properties of paddy soil (0–20 cm) under different fertilization regimes.

	pH	SOC (g·kg^{-1})	DOC (mg·L^{-1})	Fe_{ox} (mg·kg^{-1})	Al_{ox} (mg·kg^{-1})	P_{ox} (mg·kg^{-1})	TP (mg·kg^{-1})	DPS (%)	Grain yield (Mg·ha^{-1})	Seedling P uptake (kg·ha^{-1})
CK	6.29±	32.9±	251.8±	3788±	516±	45.06±	529.82±	1.05±	7.37±	15.89±

NPK	0.12b	2.2b	9.7c	314a	49a	1.30c	14.1c	0.10b	0.74b	1.78b
	6.71±	32.3±	280.2±	3916±	507±	104.96±	753.44±	2.37±	14.10±	35.90±
OM	0.13a	1.8b	14b	95a	13a	3.04a	29.0a	0.12a	0.95a	2.13a
	6.72±	40.2±	319.8±	4252±	510±	107.17±	585.45±	2.32±	14.74±	38.08±
CS	0.26a	2.5a	10.3a	283a	36a	5.77a	14.6b	0.20a	0.40a	2.58a
	6.41±	37.9±	318.1±	3763±	476±	95.19±	625.06±	2.29±	14.59±	37.09±
	0.25ab	0.6a	10.9a	181a	30a	2.09b	23.1b	0.08a	0.44a	2.50a

Different letters within a column indicate significant differences ($P < 0.05$, Tukey's test). SOC, soil organic carbon; DOC, dissolved organic carbon; Fe_{ox}, Al_{ox}, and P_{ox}, ammonium oxalate-extracted Fe, Al, and P, respectively; TP, total phosphorous; DPS, degree of phosphorous saturation; CK, control without fertilizer; NPK, chemical fertilizers input with normal NPK doses; OM, partial substitution of chemical fertilizer with organic manure; CS, partial substitution of chemical fertilizer with crop straw.

Different fertilization regimes altered the soil P fraction significantly. The proportions of soil labile P (H_2O-P, $NaHCO_3$-P_i, and $NaHCO_3$-P_o) in the OM and CS treatments were significantly higher than those in the CK and NPK treatments ($P < 0.05$, Fig. 1d). The proportions of soil residual-P were significantly lower in the fertilization treatments (NPK, OM, and CS) than in the CK treatment ($P < 0.05$, Fig. 1d). Soil labile P (H_2O-P and $NaHCO_3$-Pi) concentrations in the OM and CS were equal to or even higher than those in the NPK treatment (Table S2). The NaOH-P_i (160.74 mg·kg^{-1}) and residual-P (225.96 mg·kg^{-1}) values in the NPK treatment were significantly higher than those in other treatments ($P < 0.05$, Table S2).

The P sorption data fit the Langmuir model well, with $R^2 > 0.90$ in all treatments, showing a typical trend (i.e., increased P sorption in higher P concentration solutions, although in decreasing increments) (Fig. 1e, Table S3). The values of the P sorption isotherm parameters (Q_m and k) of the OM and CS treatments were significantly lower than those of the CK and NPK treatments, which showed that organic–inorganic fertilization decreased the P sorption capacity and P bonding energy at the sorption sites ($P < 0.05$, Table S3). Specifically, the Qm values of the OM (775.02 mg·kg^{-1}) and CS (858.39 mg·kg^{-1}) treatments were 27.12% and 19.28% lower than that of the NPK treatment, respectively (1,063.37 mg·kg^{-1}) (Table S3). Correlation analyses showed that PAC, PUE, grain yield, and seedling P uptake were negatively correlated with P sorption parameters (Q_m and k) (Fig. 1f). The above results suggest partial substitution of chemical fertilizer with manure or crop straw maintained high P availability and grain yield, with reduced chemical P fertilizer, by inhibiting soil P sorption capacity.

3.2. Soil DOM properties in the field experiment

Our results showed that DOM properties and composition could be influenced significantly by fertilization regimes (Table S4, Fig. S1). Spectral indices, such as S_R, HIX, $SUVA_{254}$, and $SUVA_{260}$ are used extensively to evaluate DOM MW, humification degree, aromaticity, and hydrophobicity, respectively (Liu et al., 2019a; Ni et al., 2022; Yeh et al., 2014). Significant decreases in S_R values were observed in the OM and CS compared with those in the CK and NPK treatments, which showed an increase in DOM MW ($P < 0.05$, Table S4). The variations in HIX, $SUVA_{254}$, and $SUVA_{260}$ values showed that DOM humification degree, aromaticity, and hydrophobicity were significantly higher in the OM and CS treatments than in the CK and NPK treatments ($P < 0.05$, Table S4). There were no significant differences in FIX index among the different fertilization regimes (Table S4).

Three fluorescent components were identified by the EEM-PARAFAC analysis of soil DOM from different fertilization regimes (Fig. S1a and b), including two humic-like components (C1 and C2) and one tyrosine-like component (C3). The tyrosine-like component (C3) was the main DOM component in the paddy soils, accounting for 65.7–78.1% of the total DOM (Fig. S1c). The highest proportions of humic-like components (C1/C2) were observed in the OM treatment (34.4%), followed by the CS treatment (27.4%), which were significantly higher than those in the CK and NPK treatments ($P < 0.05$, Fig. S1c). However, no significant differences in relative proportions of the DOM components were observed between the CK and NPK treatments.

Preprints (www.preprints.org) | NOT PEER-REVIEWED | Posted: 3 October 2023 doi:10.20944/preprints202309.2078.v1

3.3. Relationships between phosphorus sorption capacity and soil DOM properties in the field experiment

Our results showed that DOC, SOM, P_{ox} and Olsen-P were significantly and negatively correlated with P sorption parameters (Q_m and k) ($P < 0.05$, Fig. 2a). Conversely, the S_R and tyrosine-like components were significantly and positively correlated with P sorption parameters (Q_m and k), whereas the HIX, $SUVA_{254}$, $SUVA_{260}$ and humic-like components were significantly and negatively correlated with P sorption parameters (Q_m and k) ($P < 0.05$, Fig. 2b). Moreover, there was a strong correlation between the DOM properties and DOM composition (Fig. S2). Specifically, $SUVA_{254}$, $SUVA_{260}$, HIX, and the proportion of humic-like components were significantly and positively correlated, whereas S_R and the proportions of tyrosine-like components were significantly and negatively correlated with the first five indices ($P < 0.05$, Fig. S2).

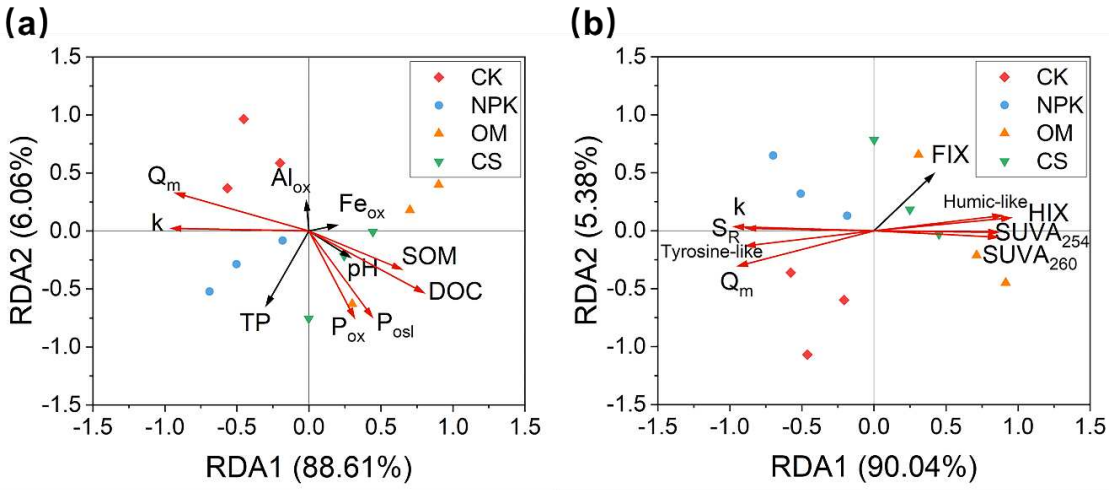

Figure 2. Redundancy analysis (RDA) showing the relationships between phosphorus (P) sorption parameters and soil properties (a) and dissolved organic matter (DOM) properties (b) under different fertilization regimes. Red and black arrows indicate the significant ($P < 0.05$) and nonsignificant ($P > 0.05$) factors, respectively. Q_m, the maximum P sorption capacity; k, P bonding energy; SOM, soil organic matter; DOC, dissolved organic matter; Fe_{ox}, Al_{ox}, and P_{ox}, ammonium oxalate-extracted Fe, Al, and P, respectively; TP, total P; S_R, the ratio of the slope (275–295 nm slope: 350–400 nm slope), with higher S_R indicating a higher molecular weight of DOM; HIX, humification index, reflecting the humification degree of DOM; FIX, fluorescence index, defined as a surrogate for the origin of DOM; $SUVA_{254}$, specific UV absorbance at 254 nm, as an indicator of aromaticity; $SUVA_{260}$, specific UV absorbance at 260 nm, as an indicator of hydrophobicity; Humic-like and tyrosine-like, proportion of humic-like substances (C1 and C2) and tyrosine-like components.

3.4. Impacts of MW-fractionated DOM on soil phosphorus sorption in the microcosm experiment

Soil P sorption experiments with different MW-fractionated DOM showed that the P sorption isotherms of soil with and without the MW-fractionated DOM fit the Langmuir model well ($R^2 > 0.94$) (Fig. 3a, b, Table 2). In the bulk soil, P was strongly adsorbed by the soil, with a P sorption maximum (Q_m) value of 1,040.09 ± 45.9 mg kg^{-1} (Table 2). MW-fractionated DOM decreased the Q_m value of paddy soil significantly ($P < 0.05$, Table 2). Specifically, when compared with that in bulk soil, the Q_m values of soil with M-HMW and S-HMW addition were reduced by 42% and 30%, respectively, whereas the Q_m values of soil with M-LMW and S-LMW addition were reduced by only 22% and 14%, respectively (Table 2). In short, the inhibition effect on soil P sorption by M-DOM was significantly greater than that of S-DOM. And the HMW-fractionated DOM inhibited soil P sorption capacity to a greater extent than the LMW-fractionated DOM by 16-20%. ($P < 0.05$, Table 2).

Preprints (www.preprints.org) | NOT PEER-REVIEWED | Posted: 3 October 2023 doi:10.20944/preprints202309.2078.v1

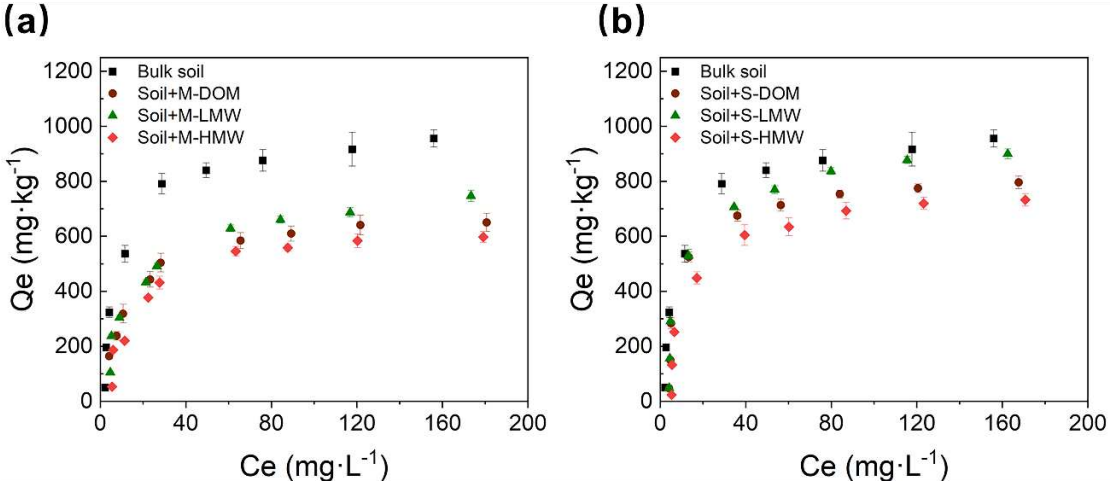

Figure 3. Phosphorous (P) sorption isotherm with the addition of different molecular weight (MW)-fractionated dissolved organic matter (DOM) from organic mature (a, M-DOM) or crop straw (b, S-DOM). M-LMW, low molecular weight fractionated DOM derived from organic manure; M-HMW, high molecular weight fractionated DOM derived from organic manure; S-LMW, low molecular weight fractionated DOM derived from crop straw; S-HMW, high molecular weight fractionated DOM derived from crop straw; Error bars show standard deviations from triplicate measurements.

Table 2. Parameters of phosphorus sorption isotherm models in the paddy soil with the addition of MW-fractionated DOM from organic mature and crop straw.

Treatment		**Langmuir model**	
	Qm (mg kg^{-1})	k (L mg^{-1})	L-R^2
Bulk soil	1040.09±45.90a	0.106±0.001a	0.98
Soil + M-DOM	696.56±18.87e	0.071±0.003b	0.99
Soil + M-LMW	807.16±7.43c	0.081±0.004b	0.97
Soil + M-HMW	600.35±19.90f	0.019±0.001c	0.97
Soil + S-DOM	777.73±11.94cd	0.008±0.001c	0.94
Soil + S-LMW	891.21±24.70b	0.022±0.011c	0.95
Soil + S-HMW	724.21±15.69de	0.006±0.001c	0.96

Different letters within a column are significantly different at $P < 0.05$. Q_m, the maximum phosphorus (P) sorption capacity; k, P bonding energy; Bulk soil, soil sample selected from the CK treatment; M-DOM, organic manure DOM; S-DOM, crop straw DOM; M-LMW, the low molecular weight fraction of M-DOM (<1 kDa); M-HMW, the high molecular weight fraction of M-DOM (1 kDa–0.45 μm); S-LMW, the low molecular weight fraction of S-DOM (<1 kDa); S-HMW, the high molecular weight fraction of S-DOM (1 kDa–0.45 μm).

3.5. Properties of MW-fractionated DOM

The DOC concentrations of S-DOM (1990.14 ± 14.3 mg L^{-1}) were nearly seven times higher than those of the M-DOM (292.4 ± 3.5 mg·L^{-1}) (Fig. 4a). In terms of DOM sources, the DOC concentrations of the M-LMW and S-LMW were 207.4 ± 4.2 and 1,477.1 ± 10.4 mg·L^{-1}, respectively, accounting for 70.9% and 74.2% of the total concentrations, respectively (Fig. 4a). The S_R values showed that the MW of M-DOM was significantly greater than that of S-DOM, and the MW of HMW-fractionated DOM was significantly larger than that of LMW-fractionated DOM ($P < 0.05$, Table S5). The humification degree, aromaticity, and hydrophobicity of the M-DOM were significantly higher than those of the S-DOM ($P < 0.05$, Fig. 4b, Table S5). The HMW-fractionated DOM of both organic fertilizers had higher humification degrees, aromaticity, and hydrophobicity than those of the LMW-fractionated DOM ($P < 0.05$, Fig. 4b, Table S5).

Preprints (www.preprints.org) | NOT PEER-REVIEWED | Posted: 3 October 2023 doi:10.20944/preprints202309.2078.v1

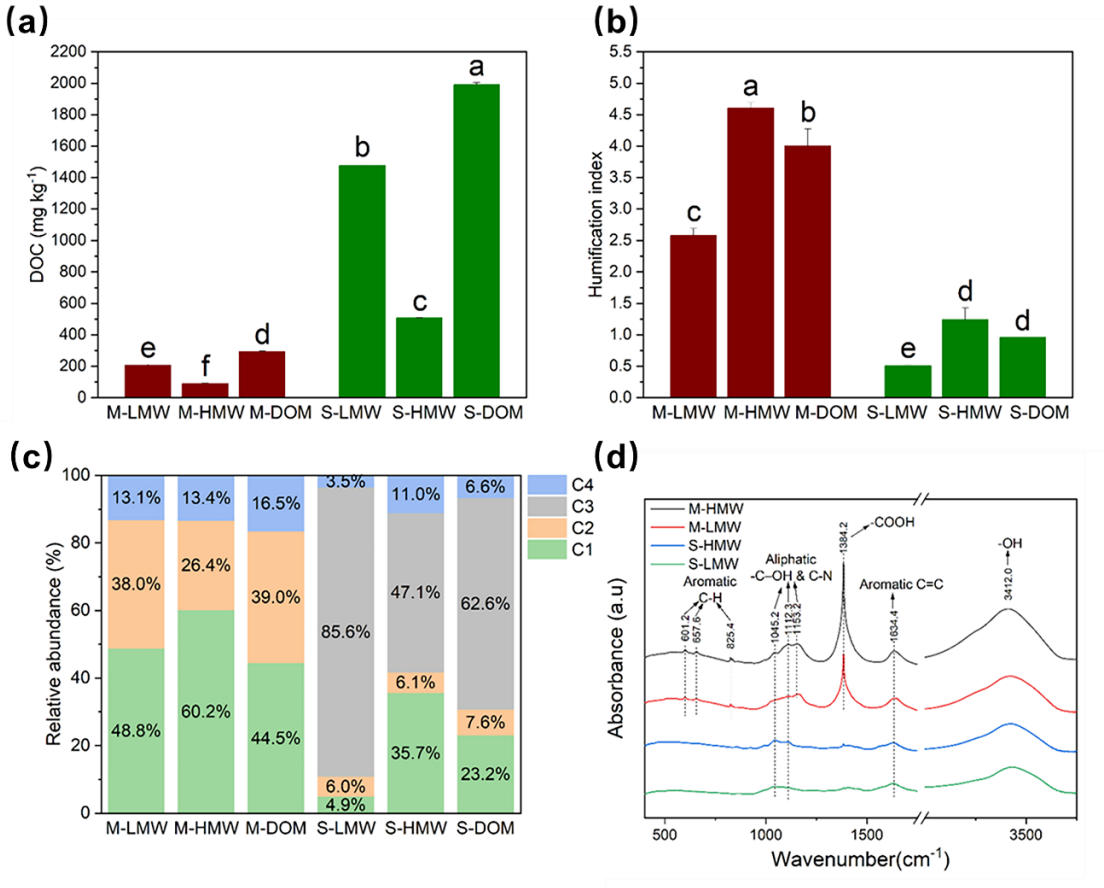

Figure 4. Properties and composition of molecular weight (MW) fractionated dissolved organic matter (DOM). (a) Dissolved organic carbon (DOC) concentrations of MW-fractionated DOM. (b) Humification index (HIX) of MW-fractionated DOM (c) The relative abundance of fluorescent components of MW-fractionated DOM. C1, C2 represent humic-like substances, C3 represents tyrosine-like component and C4 represents tryptophan-like component. (d) Fourier transform infrared (FTIR) spectra of MW-fractionated DOM. Different letters represent significant differences at $P < 0.05$ (Tukey's test). Error bars show standard deviations from triplicate measurements.

Four fluorescent components were successfully identified for the MW-fractionated DOM (Fig. S3a and b), including two humic-like components (C1 and C2), one tyrosine-like component (C3), and one tryptophan-like component (C4). As shown in Fig. 4c, humic-like components (C1 and C2) were the main components (83.5%) of M-DOM, followed by tryptophan-like materials (C4, 16.5%). In S-DOM, tyrosine-like matter (C3) had the highest proportion (62.6%), followed by humic-like substances (C1 and C2, 30.8%), and tryptophan-like material (C4, 6.6%). The proportion of the C1 component in the HMW-fractionated DOM was significantly higher than that of the LMW-fractionated DOM, regardless of their sources ($P < 0.05$, Fig. 4c). The proportion of the C2 component of M-HMW was lower than those of M-LMW and M-DOM ($P < 0.05$, Fig. 4c). In addition, in S-HMW, the proportion of tryptophan-like material (C4) was significantly higher, and the proportion of tyrosine-like matter (C3) was significantly lower, than those of the of S-LMW and S-DOM ($P < 0.05$, Fig. 4c).

FTIR spectra of MW-fractionated DOM showed that all the types contained alkanes with polar groups of –O–H, aromatic C=C, aliphatic -C-OH and C-N, and CH_x (Fig. 4d). M-HMW and M-LMW contained more aromatic C-H and –COOH groups than the S-HMW and S-LMW. Notably, compared with M-LMW, M-HMW has more carboxyl groups, aromatic substances, and benzene ring structures, similar to phenolic acid (Chen et al., 2010). S-HMW contained more carboxyl groups and aromatic substances than S-LMW (Fig. 4d).

Preprints (www.preprints.org) | NOT PEER-REVIEWED | Posted: 3 October 2023 doi:10.20944/preprints202309.2078.v1

3.6. Impacts of MW-fractionated DOM on soil microstructure and surface charge in the microcosm experiment

Soil particles with MW-fractionated DOM were generally smoother, with lower SSA and pore volume, compared with bulk soil (Fig. 5a-e). Compared with the bulk soil, the soil SSA and V_{micro} of the soil were significantly reduced with the addition of all the MW-fractionated DOM ($P < 0.05$, Fig. 5a-e). Similarly, the soil V_{total} was reduced significantly with the addition of M-HMW, S-HMW, and S-LMW ($P < 0.05$, Fig. 5a-e). M-HMW had the strongest pore blockage effect and decreased the SSA of the soil particles by 58.3%, V_{total} by 38.1%, V_{micro} by 88.6%, and V_{meso} by 31.0% (Fig. 5a-e), followed by M-LMW and S-HMW, with SSA reductions of 40.0–42.0%. The S-LMW had the lowest pore blockage effect (Fig. 5a-e). M-LMW increased the soil APS significantly, whereas the other MW-fractionated DOM had no significant effect (Fig. 5a-e). In addition, S_R was significantly positively correlated with SSA and V_{micro}, but not with V_{total}, V_{meso}, or APS (Fig. S4a-e).

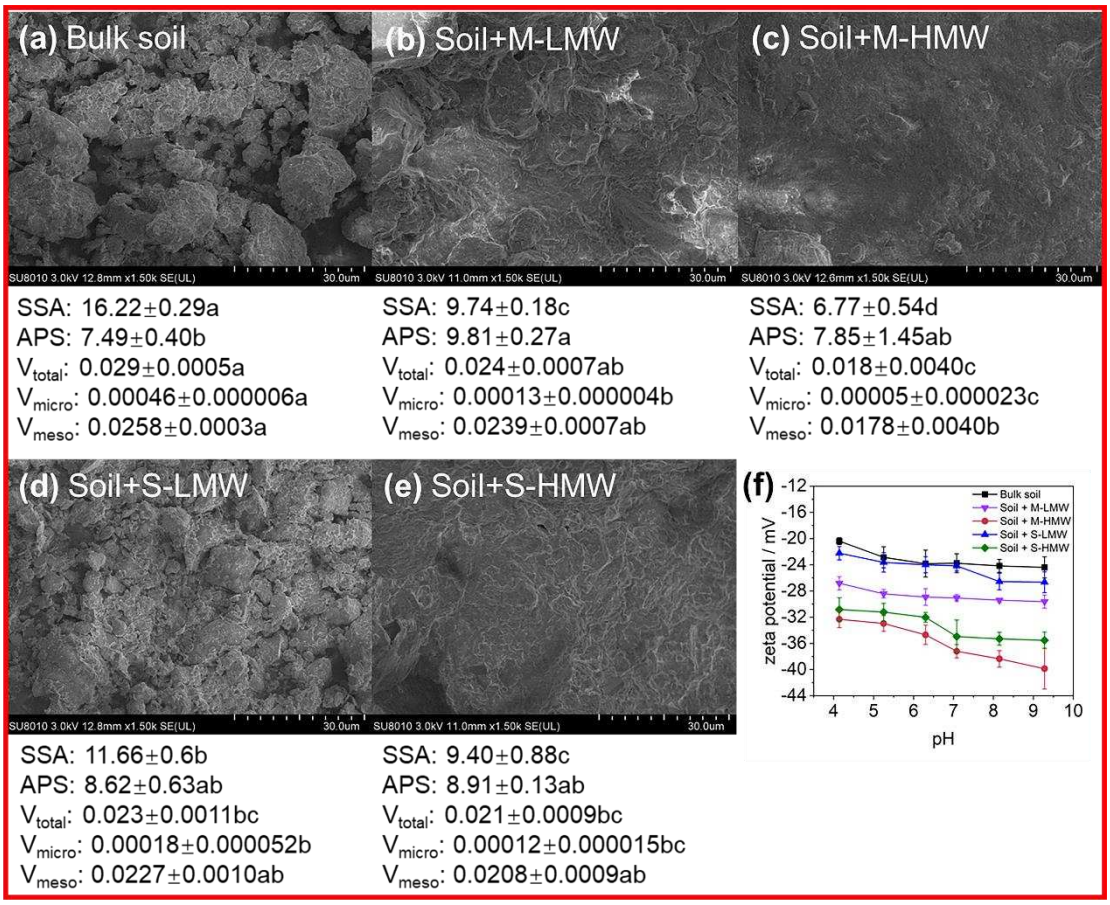

Figure 5. Scanning electron micrographs of soil with and without (bulk) the addition of molecular weight (MW) fractionated dissolved organic matter (DOM) at 1,500 × magnification (a–e). The micro-parameters showing changes in soil microstructure, including soil specific surface area (SSA, $m^2\ g^{-1}$), average pore size (APS, nm), total pore volume (V_{total}, $cm^3\ g^{-1}$), micro pore volume (V_{micro}, $cm^3\ g^{-1}$), mesoporous pore volume (V_{meso}, $cm^3\ g^{-1}$). (f) Zeta potential–pH curves of paddy soils with different MW-fractionated DOM, reflecting change in soil surface charge. Different letters represent significant differences at $P < 0.05$ (Tukey's test). Error bars show standard deviations from triplicate measurements.

The surface charge of the soil plays a critical role in the sorption process. Our results showed that the zeta potential of soil reduced with an increase in pH in laboratory experiments (Fig. 5f). The addition of MW-fractionated DOM reduced the soil zeta potential significantly (bulk soil > S-LMW > M-LMW > S-HMW > M-HMW) at the same pH ($P < 0.05$, Fig. 5f). For instance, compared with bulk soil, the soil zeta potential was reduced following the addition of M-HMW, S-HMW, M-LMW, and

Preprints (www.preprints.org) | NOT PEER-REVIEWED | Posted: 3 October 2023 doi:10.20944/preprints202309.2078.v1

S-LMW by 45.6%, 34.4%, 20.6%, and 0.7%, respectively, when the soil pH was 7. S_R was significantly positively correlated with zeta potential (Fig. S4f).

3.7. Relationships among phosphorus sorption capacity, DOM properties, and soil microstructure in the microcosm experiment

The relationships between MW, DOM properties, soil microstructure, zeta potential, and P availability in the microcosm experiment were elucidated using PLS-PM analysis (Fig. 6). The increase in MW reduced the zeta potential and thereby directly improved soil P availability ($P < 0.05$, Fig. 6a). MW had a direct positive effect on DOM properties ($P < 0.01$, Fig. 6a), and variations in DOM properties indirectly increased P availability by decreasing zeta potential ($P < 0.001$, Fig. 6a). DOM properties had direct negative effects on soil microstructure ($P < 0.001$, Fig. 6a), which also indirectly improved P availability by reducing zeta potential ($P < 0.05$, Fig. 6a). Soil microstructure and zeta potential had strong direct effects on P availability, whereas MW and DOM properties alter soil P availability mainly through indirect effects (Fig. 6b). In addition, C1 and C4 were significantly negatively correlated with Q_m, whereas C3 was significantly positively correlated with Q_m ($P < 0.01$, Table S6). C2 was significantly positively correlated with k ($P < 0.05$; Table S6).

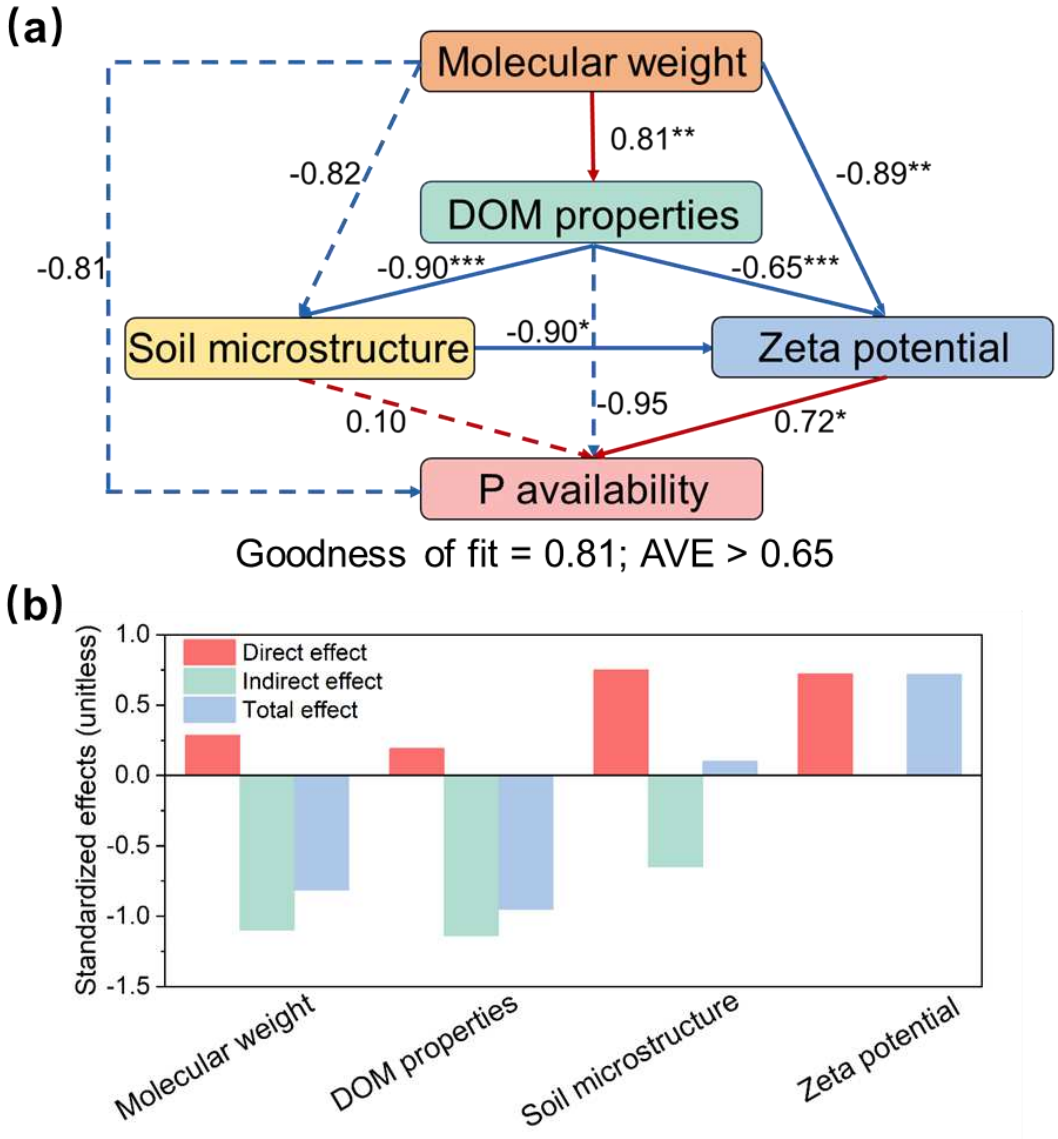

Figure 6. Cascading effect of DOM molecular weight on soil P availability. (a) Partial least squares path modelling (PLS-PM) analysis of the relationships between Molecular weight, DOM properties, soil microstructure, zeta potential, and P availability and (b) the corresponding standardized effects.

Molecular weight is characterized by the ratio of the slope (275-295nm slope: 350-400nm slope, S_R) of DOM. DOM properties include humification index (HIX), fluorescence index (FIX), $SUVA_{254}$, $SUVA_{260}$. Soil microstructure include soil specific surface area (SSA) and micro pore volume (V_{micro}). soil P availability is characterized by the maximum P sorption capacity (Q_m). Red and blue arrows indicate positive and negative correlations, respectively. Dotted lines represent pathways with non-significant effect. Numbers on the arrows indicate standardized path coefficients (* $P < 0.05$, ** $P < 0.01$, and *** $P < 0.001$).

4. Discussion

4.1. Manure and crop straw applications increased P utilization efficiency in paddy soil

Our results showed that OM and CS maintained Olsen-P, grain yields and seedling P uptake and improved PUE in paddy soil under reduced chemical P inputs (-34%). The results demonstrated that organic–inorganic fertilization increased P availability to rice, which is consistent with the findings of previous studies (Damon et al., 2014; Du et al., 2020; Qaswar et al., 2020), suggesting the importance of organic fertilizers in sustainable agriculture.

By assessing the composition of P fractions in the soil, we demonstrated that organic–inorganic fertilization increased PAC and decreased NaOH-P_i content, indicating that P availability was promoted by the addition of organic matter. The reduction in NaOH-P_i content reflects the release of P adsorbed by Al and Fe, as NaOH-P_i usually represents the P fraction adsorbed by amorphous and crystalline Al and Fe (Weng et al., 2011; Yan et al., 2017). Correlation analyses further confirmed that PAC, PUE, grain yield, and seedling P uptake were negatively correlated with the P sorption parameters (Q_m and k), indicating that organic–inorganic fertilization decreased soil P sorption capacity, and help to improve soil P availability, plant PUE, and crop yield. Although Yan et al. (2017) reported that organic–inorganic fertilization may increase the P sorption capacity of paddy soil by improving amorphous Fe/Al contents, our study showed that the amorphous Fe/Al content did not significantly differ among the treatments. In addition, the increased soil pH in the present study may facilitate the improvement of P availability, because it has been reported that increased pH can inhibit P sorption by reducing the electrical potential of mineral surfaces in acidic soils (Abdala et al., 2012; Bai et al., 2017). Overall, the results indicate that partial substitution of chemical P fertilizer with organic fertilizer reduced soil P sorption, thus maintaining high soil P availability and crop yields.

It has been reported that manure application and straw return could inhibit soil P immobilization by increasing SOM and DOC content (Kang et al., 2011; Li et al., 2022c; Weyers et al., 2017), highlighting the importance of SOM and DOC on P availability. Higher concentrations of organic matter can release more available P by competing for P sorption sites and inhibiting mineral precipitation on calcite in alkaline and acidic soils (Giesler et al., 2005; Hutchison and Hesterberg, 2004; Weyers et al., 2017; Zhu et al., 2021). Indeed, in the field experiment, we observed that the DOC content in paddy soils was negatively correlated with soil P sorption parameters (Qm and k), and positively correlated with Olsen-P content. We further analyzed the soil DOM properties and composition and observed that organic–inorganic fertilization increased soil DOM MW, humification degree, aromaticity, hydrophobicity, and humic-like components. The properties were variables predicting soil P sorption capacity. This is consistent with our previous finding that DOM humification degree and aromaticity was negatively correlated with soil P sorption (Li et al., 2022a). Therefore, the evidence from our field trials highlights the major influence of DOM in soil P sorption capacity and crop yield following organic fertilizer application, although it is still difficult to disaggregate the effects of DOM content and characteristics.

4.2. DOM properties influence soil P sorption capacity

In our field trials, DOM MW was significantly correlated with DOM properties and composition. To further clarify the importance of DOM content and properties on soil P sorption and demonstrate how MW-fractionated DOM affects P sorption, and another P sorption experiment was conducted by introducing MW-fractionated DOM into bulk soil. The results of the present study showed that both

 doi:10.20944/preprints202309.2078.v1

M-DOM and S-DOM inhibited soil P sorption capacity and that the HMW-fractionated DOM had a greater inhibitory effect on P sorption than the LMW-fractionated DOM. A similar phenomenon is observed in organic pollutant studies, in which DOM fractions reduce prometryne and pyrene sorption by binding competitively to soil sorption sites, and the reduction is more pronounced with an increase in DOM MW (Chen et al., 2010; Lin et al., 2018). Notably, in the present study, the majority of DOM derived from organic fertilizer was the LMW-fractionated DOM, which has been demonstrated to contribute weakly to P mobilization. In other words, the HMW-fractionated DOM with low DOC content probably determines the soil P sorption capacity. This may rectify the misconception that more DOC input leads to greater soil P sorption inhibition (Giesler et al., 2005; Moorberg et al., 2017; Weyers et al., 2017). The results indicate that it is inappropriate to judge the effect of organic fertilizers on P turnover based on their DOC content.

In terms of DOM properties, our results revealed that the HMW-fractionated DOM had greater humification, aromaticity, hydrophobicity and more carboxyl groups, aromatic substances, and benzene ring structures than did the LMW-fractionated DOM, and that Q_m was significantly correlated with the properties. The results demonstrate that these properties of DOM are critical in influencing P sorption behavior in paddy soil. Recent research has suggested that HMW compounds of DOM, including polycyclic aromatics, polyphenols, and carboxylic compounds, has a major affinity for iron oxides (Li et al., 2022b; Lv et al., 2016; Wang et al., 2019), which are considered to be both crucial sorbents for P and DOM in soil (Gérard, 2016; Hiemstra et al., 2013; Weng et al., 2011). Significant negative correlations between highly aromatic humic-like components (C1) and tryptophan-like components (C4) with Q_m were observed in the present study (Table S6), highlighting the potential of the substances to inhibit P sorption. Highly aromatic humic-like components (C1) were previously reported to comprise large hydrophobic compounds with a strong tendency to sorb to soil particles, minerals, and sediments (Ishii and Boyer, 2012; Sharma et al., 2017), whereas the tryptophan-like component (C4) can exert a significant chelating effect on the P released from Fe/Al phosphate minerals (Hou et al., 2018; Zhu et al., 2021). This suggests that the suppression of soil P sorption by DOM may be associated with the competition between aromatic humic acids and tryptophan for P sorption sites on the soil Fe/Al mineral surfaces. In contrast, the presence of tyrosine-like substances (C3) might increase the sorption of phosphate on soil mineral surfaces (Yeasmin et al., 2014), which is supported by the positive correlation between the proportion of tyrosine-like substances and Q_m (Fig. 2b, Table S6). Overall, we suggest that the HMW-fractionated DOM is mainly responsible for the decrease in P sorption in paddy soil owing to its stronger affinity for soil particles and Fe/Al minerals.

As mentioned above, the reduced P sorption observed in our results could be partly attributed to the competitive sorption of DOM. We assessed the soil microstructure and found following the addition of different MW-fractionated DOM, especially the HMW-fractionated DOM, soil particles were generally smoother, with a lower SSA and lower pore volumes. The phenomenon indicates that the number of available P sorption sites might be reduced because the P sorption capacity is often positively correlated with the surface sites of soil particles (Gérard, 2016; Li et al., 2022c; Wang et al., 2013). The underlying mechanism may be pore blockage due to DOM introduction (Haham et al., 2012; Lin et al., 2017). A study on herbicides also found that the addition of DOM, especially DOM with high aromaticity and large molecular weight, reduced soil SSA and pore volumes (Wu et al., 2021a). In addition, our results showed that the HMW-fractionated DOM mainly reduced soil SSA and V_{micro}, but not V_{total}, V_{meso}, or APS. Smaller soil pores may be more favorable for P sorption (Yeasmin et al., 2014). Interestingly, PLS-PM analysis indicated that the changes in soil microstructure due to DOM addition could not significantly increase soil P availability directly, but rather have an indirect effect through zeta potential (Fig. 6a). The lower zeta potential of the soil results in a smaller P adsorption capacity, owing to the electrostatic repulsion to negatively charged phosphate radicals (Wang et al., 2020). In our study, the addition of MW-fractionated DOM decreased the zeta potential of soil particles, and the soil zeta potential of the HMW-fractionated DOM treatment was lower than that of the LMW-fractionated DOM at the same pH. Because Fe/Al oxides have been reported to be the main carriers of soil variable charge (Hiemstra et al., 2013; Weng et al., 2011), the reduced zeta

potential following the addition of the HMW-fractionated DOM suggests that DOM competes for P sorption sites on soil Fe/Al oxides. Overall, the results of the present study demonstrates that DOM properties, rather than DOC content, influence soil P sorption capacity.

4.3. Importance of DOM derived from organic fertilizers on soil phosphorus availability

Our results suggest that HMW-fractionated DOM derived from organic manure and crop straw play major roles in promoting P availability mainly via competition between DOM and P for soil surface adsorption sites, decreasing the soil zeta potential, and increasing repulsion of phosphate anions. This could be attributed to more humic-like components, carboxyl groups, benzene ring structures, aromatic substances with high molecular weight, humification degree, aromaticity, and hydrophobicity. In contrast, the DOC content of organic fertilizers cannot be used to reflect their potential to improve P release from the soil. Therefore, in terms of improving P availability in paddy soils, the application of mineral fertilizers combined with organic fertilizers rich in DOM with high MW (e.g., organic manure) might be a promising approach. The targeted organic fertilizers can be further developed by adding HMW DOM.

Despite the advantage of the HMW-fractionated DOM in improving P availability, whether the HMW-fractionated DOM can effectively decrease P sorption in other soils requires further study. Moreover, the role of LMW-fractionated DOM should not be overlooked. It has been reported that LMW DOM (e.g., organic acids) has an obvious P-mobilizing ability in calcareous, neutral, and acidic soils (Hou et al., 2018; Wang et al., 2015), which was also observed in the present study. Besides, in living soils, P sorption and availability are regulated by biological processes (especially by soil microbiota) (Bi et al., 2018; Bi et al., 2020; Liu et al., 2021). However, the effects of different MWs of organic matter on the soil microbial community remain unclear. LMW DOM may be more easily utilized by microorganisms and is beneficial to microorganisms that can proliferate rapidly (r-strategist), whereas HMW organic matter may promote carbon fixation and organic P decomposition by soil microorganisms (e.g., abundant taxa) (Liu et al., 2022; Roth et al., 2019). Future research should comprehensively investigate the impacts of various MW organic matter on P availability and the impacts on soil microbiomes and plant growth.

5. Conclusions

This study emphasizes the importance of properties of DOM derived from organic fertilizers for the P availability and immobilization in paddy soil. Our field experiment and microcosm experiments demonstrated that the HMW-fractionated DOM had a greater inhibitory effect on P sorption than the LMW-fractionated DOM. The mechanism is that the HMW-fractionated DOM with unique characteristics (e.g., strong aromaticity, hydrophobicity, and richness in humic-like components, carboxyl groups, and benzene ring structures) exhibits greater suppression of soil P sorption than the LMW-fractionated DOM through site competition and charge-driven mechanisms. Overall, our findings provide a new strategy for improving PUE by regulating soil organic carbon to conserve finite P resources and reduce potential environmental pollution. This would further help in organic fertilizer development and application in sustainably managed agricultural systems to sustain high P bioavailability levels from decreasing mineral P fertilization.

Supplementary Materials:

Acknowledgments: This work was supported by the National Natural Science Foundation of China (No. 42077088) and Zhejiang Province "Agriculture, Rural Areas, Rural People and Nine Institutions" Science and Technology Collaboration Program (2023SNJF039). Xipeng Liu was supported by a scholarship from the China Scholarship Council. We thank Dr. Liang Ni (AES of Zhejiang University) for his help in field experiment management and soil sample collection.

Author contributions: Haibo Wang: Visualization, Investigation, Methodology, Conceptualization, Resources, Software, Writing – original draft, Writing – review & editing. **Xipeng Liu:** Visualization, Conceptualization, Resources, Writing – review & editing. **Bingjie Jin:** Resources, Writing – review & editing. **Yucheng Shu:** Formal analysis, Methodology. **Chengliang Sun:** Conceptualization, Writing – review & editing. **Yongguan Zhu:**

Conceptualization, Writing – review & editing. **Xianyong Lin:** Conceptualization, Supervision, Project administration, Funding acquisition, Writing – review & editing.

Abbreviations

DOM, dissolved organic matter; P, phosphorous; DOC, dissolved organic carbon; PUE, P fertilizer use efficiency; MW, molecular weight; SOC, soil organic carbon; TP, total phosphorous; PAC, phosphorus activation coefficient; DPS, degree of phosphorus saturation; Q_m, the maximum P sorption capacity; k, P bonding energy constant; P_i, inorganic phosphorous; P_o, organic phosphorous; LMW, low molecular weight; HMW, high molecular weight; UV-vis, ultraviolet visible; EEM-PARAFAC, excitation-emission matrices-parallel factor analysis; HIX, humification index; FIX, fluorescence index; $SUVA_{254}$ and $SUVA_{260}$, specific Ultra Violet absorbance at 254 nm and 260 nm; SSA, specific surface area; APS, average pore size; V_{total}, total pore volume; V_{micro}, micropore volume; V_{meso}, mesopore volume; FT-IR, Fourier transform infrared spectroscopy; RDA, redundancy analysis.

References

1. Abdala, D.B., Ghosh, A.K., da Silva, I.R., de Novais, R.F., Alvarez Venegas, V.H., 2012. Phosphorus saturation of a tropical soil and related P leaching caused by poultry litter addition. Agriculture, Ecosystems & Environment 162, 15-23. https://doi.org/10.1016/j.agee.2012.08.004.
2. Amaral, V., Graeber, D., Calliari, D., Alonso, C., 2016. Strong linkages between DOM optical properties and main clades of aquatic bacteria. Limnology and Oceanography 61, 906-918. https://doi.org/10.1002/lno.10258.
3. Bai, J., Ye, X., Jia, J., Zhang, G., Zhao, Q., Cui, B., Liu, X., 2017. Phosphorus sorption-desorption and effects of temperature, pH and salinity on phosphorus sorption in marsh soils from coastal wetlands with different flooding conditions. Chemosphere 188, 677-688. https://doi.org/10.1016/j.chemosphere.2017.08.117.
4. Bi, Q.-F., Zheng, B.-X., Lin, X.-Y., Li, K.-J., Liu, X.-P., Hao, X.-L., Zhang, H., Zhang, J.-B., Jaisi, D.P., Zhu, Y.-G., 2018. The microbial cycling of phosphorus on long-term fertilized soil: Insights from phosphate oxygen isotope ratios. Chemical Geology 483, 56-64. https://doi.org/10.1016/j.chemgeo.2018.02.013.
5. Bi, Q.F., Li, K.J., Zheng, B.X., Liu, X.P., Li, H.Z., Jin, B.J., Ding, K., Yang, X.R., Lin, X.Y., Zhu, Y.G., 2020. Partial replacement of inorganic phosphorus (P) by organic manure reshapes phosphate mobilizing bacterial community and promotes P bioavailability in a paddy soil. Sci Total Environ 703, 134977. https://doi.org/10.1016/j.scitotenv.2019.134977.
6. Bolan, N.S., Adriano, D.C., Kunhikrishnan, A., James, T., McDowell, R., Senesi, N., 2011. Dissolved Organic Matter. 110, 1-75. https://doi.org/10.1016/b978-0-12-385531-2.00001-3
7. Borges, B.M.M.N., Abdala, D.B., Souza, M.F.d., Viglio, L.M., Coelho, M.J.A., Pavinato, P.S., Franco, H.C.J., 2019. Organomineral phosphate fertilizer from sugarcane byproduct and its effects on soil phosphorus availability and sugarcane yield. Geoderma 339, 20-30. https://doi.org/10.1016/j.geoderma.2018.12.036.
8. Chasse, A.W., Ohno, T., 2016. Higher Molecular Mass Organic Matter Molecules Compete with Orthophosphate for Adsorption to Iron (Oxy)hydroxide. Environ Sci Technol 50, 7461-7469. https://doi.org/10.1021/acs.est.6b01582.
9. Chen, G., Lin, C., Chen, L., Yang, H., 2010. Effect of size-fractionation dissolved organic matter on the mobility of prometryne in soil. Chemosphere 79, 1046-1055. https://doi.org/10.1016/j.chemosphere.2010.03.038.
10. Cong, P.T., Merckx, R., 2005. Improving phosphorus availability in two upland soils of Vietnam using Tithonia diversifolia H. Plant and Soil 269, 11-23. https://doi.org/10.1007/s11104-004-1791-1.
11. Cordell, D., Drangert, J.-O., White, S., 2009. The story of phosphorus: Global food security and food for thought. Global Environmental Change 19, 292-305. https://doi.org/10.1016/j.gloenvcha.2008.10.009.
12. Cordell, D., White, S., 2014. Life's Bottleneck: Sustaining the World's Phosphorus for a Food Secure Future. Annual Review of Environment and Resources 39, 161-188. https://doi.org/10.1146/annurev-environ-010213-113300.
13. Damon, P.M., Bowden, B., Rose, T., Rengel, Z., 2014. Crop residue contributions to phosphorus pools in agricultural soils: A review. Soil Biology and Biochemistry 74, 127-137. https://doi.org/10.1016/j.soilbio.2014.03.003.

14. Deng, Y., Weng, L., Li, Y., Ma, J., Chen, Y., 2019. Understanding major NOM properties controlling its interactions with phosphorus and arsenic at goethite-water interface. Water Res 157, 372-380. https://doi.org/10.1016/j.watres.2019.03.077.
15. Du, Y., Cui, B., zhang, Q., Wang, Z., Sun, J., Niu, W., 2020. Effects of manure fertilizer on crop yield and soil properties in China: A meta-analysis. Catena 193. https://doi.org/10.1016/j.catena.2020.104617.
16. Ge, X., Wang, L., Zhang, W., Putnis, C.V., 2020. Molecular Understanding of Humic Acid-Limited Phosphate Precipitation and Transformation. Environ Sci Technol 54, 207-215. https://doi.org/10.1021/acs.est.9b05145.
17. Gérard, F., 2016. Clay minerals, iron/aluminum oxides, and their contribution to phosphate sorption in soils — A myth revisited. Geoderma 262, 213-226. https://doi.org/10.1016/j.geoderma.2015.08.036.
18. Giesler, R., Andersson, T., Lövgren, L., Persson, P., 2005. Phosphate Sorption in Aluminum- and Iron-Rich Humus Soils. Soil Science Society of America Journal 69, 77-86. https://doi.org/10.2136/sssaj2005.0077a.
19. Haham, H., Oren, A., Chefetz, B., 2012. Insight into the role of dissolved organic matter in sorption of sulfapyridine by semiarid soils. Environ Sci Technol 46, 11870-11877. https://doi.org/10.1021/es303189f.
20. Hawkins, J.M.B., Vermeiren, C., Blackwell, M.S.A., Darch, T., Granger, S.J., Dunham, S.J., Hernandez-Allica, J., Smolders, E., McGrath, S., 2022. The effect of soil organic matter on long-term availability of phosphorus in soil: Evaluation in a biological P mining experiment. Geoderma 423. https://doi.org/10.1016/j.geoderma.2022.115965.
21. Hedley, M.J., Stewart, J.W.B., Chauhan, B.S., 1982. Changes in Inorganic and Organic Soil Phosphorus Fractions Induced by Cultivation Practices and by Laboratory Incubations. Soil Science Society of America Journal 46, 970-976. https://doi.org/https://doi.org/10.2136/sssaj1982.03615995004600050017x.
22. Helms, J.R., Stubbins, A., Ritchie, J.D., Minor, E.C., Kieber, D.J., Mopper, K., 2008. Absorption spectral slopes and slope ratios as indicators of molecular weight, source, and photobleaching of chromophoric dissolved organic matter. Limnology and Oceanography 53, 955-969. https://doi.org/10.4319/lo.2008.53.3.0955.
23. Hiemstra, T., Mia, S., Duhaut, P.B., Molleman, B., 2013. Natural and pyrogenic humic acids at goethite and natural oxide surfaces interacting with phosphate. Environ Sci Technol 47, 9182-9189. https://doi.org/10.1021/es400997n.
24. Hou, E., Tang, S., Chen, C., Kuang, Y., Lu, X., Heenan, M., Wen, D., 2018. Solubility of phosphorus in subtropical forest soils as influenced by low-molecular organic acids and key soil properties. Geoderma 313, 172-180. https://doi.org/10.1016/j.geoderma.2017.10.039.
25. Hunt, J.F., Ohno, T., He, Z., Honeycutt, C.W., Dail, D.B., 2007. Inhibition of phosphorus sorption to goethite, gibbsite, and kaolin by fresh and decomposed organic matter. Biology and Fertility of Soils 44, 277-288. https://doi.org/10.1007/s00374-007-0202-1.
26. Hutchison, K.J., Hesterberg, D., 2004. Dissolution of phosphate in a phosphorus-enriched ultisol as affected by microbial reduction. J Environ Qual 33, 1793-1802. https://doi.org/10.2134/jeq2004.1793.
27. Ishii, S.K., Boyer, T.H., 2012. Behavior of reoccurring PARAFAC components in fluorescent dissolved organic matter in natural and engineered systems: a critical review. Environ Sci Technol 46, 2006-2017. https://doi.org/10.1021/es2043504.
28. Jalali, M., Jalali, M., 2022. Effect of Low-Molecular-Weight Organic Acids on the Release of Phosphorus from Amended Calcareous Soils: Experimental and Modeling. Journal of Soil Science and Plant Nutrition 22, 4179-4193. https://doi.org/10.1007/s42729-022-01017-1.
29. Kang, J., Amoozegar, A., Hesterberg, D., Osmond, D.L., 2011. Phosphorus leaching in a sandy soil as affected by organic and inorganic fertilizer sources. Geoderma 161, 194-201. https://doi.org/10.1016/j.geoderma.2010.12.019.
30. Lapierre, J.F., del Giorgio, P.A., 2014. Partial coupling and differential regulation of biologically and photochemically labile dissolved organic carbon across boreal aquatic networks. Biogeosciences 11, 5969-5985. https://doi.org/10.5194/bg-11-5969-2014.
31. Li, K., Bi, Q., Liu, X., Wang, H., Sun, C., Zhu, Y., Lin, X., 2022a. Unveiling the role of dissolved organic matter on phosphorus sorption and availability in a 5-year manure amended paddy soil. Sci Total Environ 838, 155892. https://doi.org/10.1016/j.scitotenv.2022.155892.
32. Li, Y., Gong, X., Sun, Y., Shu, Y., Niu, D., Ye, H., 2022b. High molecular weight fractions of dissolved organic matter (DOM) determined the adsorption and electron transfer capacity of DOM on iron minerals. Chemical Geology 604, 120907. https://doi.org/https://doi.org/10.1016/j.chemgeo.2022.120907.

33. Li, Y., Wang, J., Shao, M., 2022c. Earthworm inoculation and straw return decrease the phosphorus adsorption capacity of soils in the Loess region, China. J Environ Manage 312, 114921. https://doi.org/10.1016/j.jenvman.2022.114921.
34. Lin, B., Hua, M., Zhang, Y., Zhang, W., Lv, L., Pan, B., 2017. Effects of organic acids of different molecular size on phosphate removal by HZO-201 nanocomposite. Chemosphere 166, 422-430. https://doi.org/10.1016/j.chemosphere.2016.09.104.
35. Lin, H., Xia, X., Bi, S., Jiang, X., Wang, H., Zhai, Y., Wen, W., 2018. Quantifying Bioavailability of Pyrene Associated with Dissolved Organic Matter of Various Molecular Weights to Daphnia magna. Environ Sci Technol 52, 644-653. https://doi.org/10.1021/acs.est.7b05520.
36. Liu, C., Li, Z., Berhe, A.A., Xiao, H., Liu, L., Wang, D., Peng, H., Zeng, G., 2019a. Characterizing dissolved organic matter in eroded sediments from a loess hilly catchment using fluorescence EEM-PARAFAC and UV–Visible absorption: Insights from source identification and carbon cycling. Geoderma 334, 37-48. https://doi.org/10.1016/j.geoderma.2018.07.029.
37. Liu, W., Ling, N., Luo, G., Guo, J., Zhu, C., Xu, Q., Liu, M., Shen, Q., Guo, S., 2021. Active phoD-harboring bacteria are enriched by long-term organic fertilization. Soil Biology and Biochemistry 152, 108071. https://doi.org/10.1016/j.soilbio.2020.108071.
38. Liu, X., Wang, H., Wu, Y., Bi, Q., Ding, K., Lin, X., 2022. Manure application effects on subsoils: Abundant taxa initiate the diversity reduction of rare bacteria and community functional alterations. Soil Biology and Biochemistry 174. https://doi.org/10.1016/j.soilbio.2022.108816.
39. Liu, X.P., Bi, Q.F., Qiu, L.L., Li, K.J., Yang, X.R., Lin, X.Y., 2019b. Increased risk of phosphorus and metal leaching from paddy soils after excessive manure application: Insights from a mesocosm study. Sci Total Environ 666, 778-785. https://doi.org/10.1016/j.scitotenv.2019.02.072.
40. Liu, Y., Zhu, Z.Q., He, X.S., Yang, C., Du, Y.Q., Huang, Y.D., Su, P., Wang, S., Zheng, X.X., Xue, Y.J., 2018. Mechanisms of rice straw biochar effects on phosphorus sorption characteristics of acid upland red soils. Chemosphere 207, 267-277. https://doi.org/10.1016/j.chemosphere.2018.05.086.
41. Lv, J., Zhang, S., Wang, S., Luo, L., Cao, D., Christie, P., 2016. Molecular-Scale Investigation with ESI-FT-ICR-MS on Fractionation of Dissolved Organic Matter Induced by Adsorption on Iron Oxyhydroxides. Environ Sci Technol 50, 2328-2336. https://doi.org/10.1021/acs.est.5b04996.
42. Mastný, J., Kaštovská, E., Bárta, J., Chroňáková, A., Borovec, J., Šantrůčková, H., Urbanová, Z., Edwards, K.R., Picek, T., 2018. Quality of DOC produced during litter decomposition of peatland plant dominants. Soil Biology and Biochemistry 121, 221-230. https://doi.org/10.1016/j.soilbio.2018.03.018.
43. McKnight, D.M., Boyer, E.W., Westerhoff, P.K., Doran, P.T., Kulbe, T., Andersen, D.T., 2001. Spectrofluorometric characterization of dissolved organic matter for indication of precursor organic material and aromaticity. Limnology and Oceanography 46, 38-48. https://doi.org/https://doi.org/10.4319/lo.2001.46.1.0038.
44. Mekonnen, M.M., Hoekstra, A.Y., 2018. Global Anthropogenic Phosphorus Loads to Freshwater and Associated Grey Water Footprints and Water Pollution Levels: A High-Resolution Global Study. Water Resources Research 54, 345-358. https://doi.org/10.1002/2017wr020448.
45. Moorberg, C.J., Vepraskas, M.J., Niewhoener, C.P., 2017. Phosphorus Dynamics Near Bald Cypress Roots in a Restored Wetland. Soil Science Society of America Journal 81, 1652-1660. https://doi.org/10.2136/sssaj2017.07.0228.
46. Nebbioso, A., Piccolo, A., 2013. Molecular characterization of dissolved organic matter (DOM): a critical review. Anal Bioanal Chem 405, 109-124. https://doi.org/10.1007/s00216-012-6363-2.
47. Nelson, D.W., Sommers, L.E., 1996. Total Carbon, Organic Carbon, and Organic Matter. Methods of Soil Analysis, 961-1010. https://doi.org/https://doi.org/10.2136/sssabookser5.3.c34.
48. Ni, Z., Huang, D., Xiao, M., Liu, X., Wang, S., 2022. Molecular weight driving bioavailability and intrinsic degradation mechanisms of dissolved organic phosphorus in lake sediment. Water Res 210, 117951. https://doi.org/10.1016/j.watres.2021.117951.
49. Nobile, C.M., Bravin, M.N., Becquer, T., Paillat, J.M., 2020. Phosphorus sorption and availability in an andosol after a decade of organic or mineral fertilizer applications: Importance of pH and organic carbon modifications in soil as compared to phosphorus accumulation. Chemosphere 239, 124709. https://doi.org/10.1016/j.chemosphere.2019.124709.
50. Olsen, S.R., 1954. Estimation of available phosphorus in soils by extraction with sodium bicarbonate.

51. Panettieri, M., Guigue, J., Chemidlin Prevost-Bouré, N., Thévenot, M., Lévêque, J., Le Guillou, C., Maron, P.-A., Santoni, A.-L., Ranjard, L., Mounier, S., Menasseri, S., Viaud, V., Mathieu, O., 2020. Grassland-cropland rotation cycles in crop-livestock farming systems regulate priming effect potential in soils through modulation of microbial communities, composition of soil organic matter and abiotic soil properties. Agriculture, Ecosystems & Environment 299. https://doi.org/10.1016/j.agee.2020.106973.
52. Perassi, I., Borgnino, L., 2014. Adsorption and surface precipitation of phosphate onto CaCO3–montmorillonite: effect of pH, ionic strength and competition with humic acid. Geoderma 232-234, 600-608. https://doi.org/10.1016/j.geoderma.2014.06.017.
53. Pitta, E., Zeri, C., 2021. The impact of combining data sets of fluorescence excitation - emission matrices of dissolved organic matter from various aquatic sources on the information retrieved by PARAFAC modeling. Spectrochim Acta A Mol Biomol Spectrosc 258, 119800. https://doi.org/10.1016/j.saa.2021.119800.
54. Qaswar, M., Jing, H., Ahmed, W., Dongchu, L., Shujun, L., Lu, Z., Cai, A., Lisheng, L., Yongmei, X., Jusheng, G., Huimin, Z., 2020. Yield sustainability, soil organic carbon sequestration and nutrients balance under long-term combined application of manure and inorganic fertilizers in acidic paddy soil. Soil and Tillage Research 198. https://doi.org/10.1016/j.still.2019.104569.
55. Romanyà, J., Blanco-Moreno, J.M., Sans, F.X., 2017. Phosphorus mobilization in low-P arable soils may involve soil organic C depletion. Soil Biology and Biochemistry 113, 250-259. https://doi.org/10.1016/j.soilbio.2017.06.015.
56. Romero, C.M., Engel, R.E., D'Andrilli, J., Chen, C., Zabinski, C., Miller, P.R., Wallander, R., 2017. Bulk optical characterization of dissolved organic matter from semiarid wheat-based cropping systems. Geoderma 306, 40-49. https://doi.org/10.1016/j.geoderma.2017.06.029.
57. Roth, V.-N., Lange, M., Simon, C., Hertkorn, N., Bucher, S., Goodall, T., Griffiths, R.I., Mellado-Vázquez, P.G., Mommer, L., Oram, N.J., Weigelt, A., Dittmar, T., Gleixner, G., 2019. Persistence of dissolved organic matter explained by molecular changes during its passage through soil. Nature Geoscience 12, 755-761. https://doi.org/10.1038/s41561-019-0417-4.
58. Ryan, K.A., Palacios, L.C., Encina, F., Graeber, D., Osorio, S., Stubbins, A., Woelfl, S., Nimptsch, J., 2022. Assessing inputs of aquaculture-derived nutrients to streams using dissolved organic matter fluorescence. Sci Total Environ 807, 150785. https://doi.org/10.1016/j.scitotenv.2021.150785.
59. Sharma, P., Laor, Y., Raviv, M., Medina, S., Saadi, I., Krasnovsky, A., Vager, M., Levy, G.J., Bar-Tal, A., Borisover, M., 2017. Compositional characteristics of organic matter and its water-extractable components across a profile of organically managed soil. Geoderma 286, 73-82. https://doi.org/10.1016/j.geoderma.2016.10.014.
60. Stedmon, C.A., Bro, R., 2008. Characterizing dissolved organic matter fluorescence with parallel factor analysis: a tutorial. Limnology and Oceanography: Methods 6, 572-579. https://doi.org/https://doi.org/10.4319/lom.2008.6.572b.
61. Stedmon, C.A., Markager, S., 2005. Resolving the variability in dissolved organic matter fluorescence in a temperate estuary and its catchment using PARAFAC analysis. Limnology and Oceanography 50, 686-697. https://doi.org/https://doi.org/10.4319/lo.2005.50.2.0686.
62. Ström, L., Owen, A.G., Godbold, D.L., Jones, D.L., 2002. Organic acid mediated P mobilization in the rhizosphere and uptake by maize roots. Soil Biology and Biochemistry 34, 703-710. https://doi.org/https://doi.org/10.1016/S0038-0717(01)00235-8.
63. Takahashi, Y., Katoh, M., 2022. Root response and phosphorus uptake with enhancement in available phosphorus level in soil in the presence of water-soluble organic matter deriving from organic material. J Environ Manage 322, 116038. https://doi.org/10.1016/j.jenvman.2022.116038.
64. Teng, Z., Zhu, J., Shao, W., Zhang, K., Li, M., Whelan, M.J., 2020. Increasing plant availability of legacy phosphorus in calcareous soils using some phosphorus activators. J Environ Manage 256, 109952. https://doi.org/10.1016/j.jenvman.2019.109952.
65. Tiessen, H., Moir, J.O., 1993. Characterization of available P by sequential extraction. Soil Sampling and Methods of Analysis, 75-86.
66. Van Vuuren, D.P., Bouwman, A.F., Beusen, A.H.W., 2010. Phosphorus demand for the 1970–2100 period: A scenario analysis of resource depletion. Global Environmental Change 20, 428-439. https://doi.org/10.1016/j.gloenvcha.2010.04.004.

67. Wang, P., Li, D., Fan, X., Hu, B., Wang, X., 2020. Sorption and desorption behaviors of triphenyl phosphate (TPhP) and its degradation intermediates on aquatic sediments. J Hazard Mater 385, 121574. https://doi.org/10.1016/j.jhazmat.2019.121574.
68. Wang, X., Li, W., Harrington, R., Liu, F., Parise, J.B., Feng, X., Sparks, D.L., 2013. Effect of ferrihydrite crystallite size on phosphate adsorption reactivity. Environ Sci Technol 47, 10322-10331. https://doi.org/10.1021/es401301z.
69. Wang, Y., Chen, X., Whalen, J.K., Cao, Y., Quan, Z., Lu, C., Shi, Y., 2015. Kinetics of inorganic and organic phosphorus release influenced by low molecular weight organic acids in calcareous, neutral and acidic soils. Journal of Plant Nutrition and Soil Science 178, 555-566. https://doi.org/10.1002/jpln.201500047.
70. Wang, Y., Zhang, Z., Han, L., Sun, K., Jin, J., Yang, Y., Yang, Y., Hao, Z., Liu, J., Xing, B., 2019. Preferential molecular fractionation of dissolved organic matter by iron minerals with different oxidation states. Chemical Geology 520, 69-76. https://doi.org/10.1016/j.chemgeo.2019.05.003.
71. Weng, L., Vega, F.A., Van Riemsdijk, W.H., 2011. Competitive and synergistic effects in pH dependent phosphate adsorption in soils: LCD modeling. Environ Sci Technol 45, 8420-8428. https://doi.org/10.1021/es201844d.
72. Weyers, E., Strawn, D.G., Peak, D., Baker, L.L., 2017. Inhibition of phosphorus sorption on calcite by dairy manure-sourced DOC. Chemosphere 184, 99-105. https://doi.org/10.1016/j.chemosphere.2017.05.141.
73. Wu, C., An, W., Liu, Z., Lin, J., Qian, Z., Xue, S., 2020. The effects of biochar as the electron shuttle on the ferrihydrite reduction and related arsenic (As) fate. J Hazard Mater 390, 121391. https://doi.org/10.1016/j.jhazmat.2019.121391.
74. Wu, D., Ren, C., Wu, C., Li, Y., Deng, X., Li, Q., 2021a. Mechanisms by which different polar fractions of dissolved organic matter affect sorption of the herbicide MCPA in ferralsol. J Hazard Mater 416, 125774. https://doi.org/10.1016/j.jhazmat.2021.125774.
75. Wu, Q., Zhang, S., Zhu, P., Huang, S., Wang, B., Zhao, L., Xu, M., 2017. Characterizing differences in the phosphorus activation coefficient of three typical cropland soils and the influencing factors under long-term fertilization. PLoS One 12, e0176437. https://doi.org/10.1371/journal.pone.0176437.
76. Wu, Y., Wang, C., Wang, S., An, J., Liang, D., Zhao, Q., Tian, L., Wu, Y., Wang, X., Li, N., 2021b. Graphite accelerate dissimilatory iron reduction and vivianite crystal enlargement. Water Res 189, 116663. https://doi.org/10.1016/j.watres.2020.116663.
77. Xu, H., Guo, L., 2017. Molecular size-dependent abundance and composition of dissolved organic matter in river, lake and sea waters. Water Res 117, 115-126. https://doi.org/10.1016/j.watres.2017.04.006.
78. Yamashita, Y., Scinto, L.J., Maie, N., Jaffé, R., 2010. Dissolved Organic Matter Characteristics Across a Subtropical Wetland's Landscape: Application of Optical Properties in the Assessment of Environmental Dynamics. Ecosystems 13, 1006-1019. https://doi.org/10.1007/s10021-010-9370-1.
79. Yan, X., Wang, D., Zhang, H., Zhang, G., Wei, Z., 2013. Organic amendments affect phosphorus sorption characteristics in a paddy soil. Agriculture, Ecosystems & Environment 175, 47-53. https://doi.org/10.1016/j.agee.2013.05.009.
80. Yan, X., Wei, Z., Hong, Q., Lu, Z., Wu, J., 2017. Phosphorus fractions and sorption characteristics in a subtropical paddy soil as influenced by fertilizer sources. Geoderma 295, 80-85. https://doi.org/10.1016/j.geoderma.2017.02.012.
81. Yang, X., Chen, X., Yang, X., 2019. Effect of organic matter on phosphorus adsorption and desorption in a black soil from Northeast China. Soil and Tillage Research 187, 85-91. https://doi.org/10.1016/j.still.2018.11.016.
82. Yeasmin, S., Singh, B., Kookana, R.S., Farrell, M., Sparks, D.L., Johnston, C.T., 2014. Influence of mineral characteristics on the retention of low molecular weight organic compounds: a batch sorption-desorption and ATR-FTIR study. J Colloid Interface Sci 432, 246-257. https://doi.org/10.1016/j.jcis.2014.06.036.
83. Yeh, Y.L., Yeh, K.J., Hsu, L.F., Yu, W.C., Lee, M.H., Chen, T.C., 2014. Use of fluorescence quenching method to measure sorption constants of phenolic xenoestrogens onto humic fractions from sediment. J Hazard Mater 277, 27-33. https://doi.org/10.1016/j.jhazmat.2014.03.057.
84. Yuan, Y., Tang, C., Jin, Y., Cheng, K., Yang, F., 2022. Contribution of exogenous humic substances to phosphorus availability in soil-plant ecosystem: A review. Critical Reviews in Environmental Science and Technology, 1-18. https://doi.org/10.1080/10643389.2022.2120317.

85. Zhang, S., Wang, L., Chen, S., Fan, B., Huang, S., Chen, Q., 2022. Enhanced phosphorus mobility in a calcareous soil with organic amendments additions: Insights from a long term study with equal phosphorus input. J Environ Manage 306, 114451. https://doi.org/10.1016/j.jenvman.2022.114451.
86. Zhu, H., Bing, H., Wu, Y., Sun, H., Zhou, J., 2021. Low molecular weight organic acids regulate soil phosphorus availability in the soils of subalpine forests, eastern Tibetan Plateau. Catena 203. https://doi.org/10.1016/j.catena.2021.105328.
87. Zhu, J., Li, M., Whelan, M., 2018. Phosphorus activators contribute to legacy phosphorus availability in agricultural soils: A review. Sci Total Environ 612, 522-537. https://doi.org/10.1016/j.scitotenv.2017.08.095.
88. Zou, T., Zhang, X., Davidson, E.A., 2022. Global trends of cropland phosphorus use and sustainability challenges. Nature. https://doi.org/10.1038/s41586-022-05220-z.
89. Zsolnay, A., Baigar, E., Jimenez, M., Steinweg, B., Saccomandi, F., 1999. Differentiating with fluorescence spectroscopy the sources of dissolved organic matter in soils subjected to drying. Chemosphere 38, 45-50. https://doi.org/https://doi.org/10.1016/S0045-6535(98)00166-0.